On stress oscillation in MPM simulations involving one or two phases

Gonzalez Acosta, Leon; Zheng, Xiangcou; Vardon, Phil; Hicks, Michael; Pisano, Federico

Important note
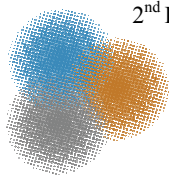To cite this publication, please use the final published version (if applicable).
Please check the document version above.

Anura3D

MPM Research Community

On stress oscillation in MPM simulations involving one or two phases

J. L. González Acosta[1,*], X. Zheng[1], P. J. Vardon[1], M. A. Hicks[1], F. Pisanò[1]

[1]Geo-Engineering Section, Delft University of Technology, Delft, The Netherlands

* E-mail: J.L.GonzalezAcosta-1@tudelft.nl

ABSTRACT

Stress oscillations in the material point method (MPM) are one of the major reasons unrealistic results are obtained. In this paper an investigation of the stress oscillations occurring when using one- and two-phase approaches is performed. Specifically, an axisymmetric benchmark and a two-dimensional plane strain problem are used to demonstrate and investigate the oscillations. Furthermore, a partially reduced integration combined with the GIMP technique (GIMP-R) is implemented to reduce large oscillations.

KEY WORDS: Hydro-mechanical; MPM; Stress oscillations

INTRODUCTION

The material point method (MPM) is a numerical technique that has been gaining recognition in the geotechnical field because of its ability to simulate problems in which large deformations occur, such as slope failure. Moreover, since MPM shares many similarities with the finite element (FE) framework, most of the enhancements developed for FE can be included in MPM simulations. Unfortunately, since MPM uses the locations of the material points to perform integration and recover stresses, inaccurate results can be obtained (e.g. stress oscillations), and such inaccuracies can be even greater in hydro-mechanical problems because of the presence of a (nearly) incompressible pore fluid. In this paper, the issues regarding stress oscillation using one-phase and two-phase MPM are studied using an axisymmetric benchmark and a two-dimensional plane strain problem. Also, an investigation of a new procedure to reduce the inaccuracies, namely GIMP-R, is carried out.

Stress oscillations in MPM have been mentioned by previous researchers (Steffen et al., 2008b; Bardenhagen, 2002; Gonzalez Acosta et al., 2017), but, although some solutions to it have been proposed (Bardenhagen and Kober, 2004; Steffen et al., 2008a), inaccuracies still persist. In literature, the most critical issue causing stress oscillations is typically associated with cell crossing, but this is not the only cause.

Another important reason for the occurrence of stress oscillations, in particular in implicit solutions, is the material point position (Gonzalez Acosta et al., 2017). The effect of the material point locations inside elements is seldom mentioned, but the consequences can be significant. Moreover, oscillations increase in two-phase problems when the undrained-incompressible limit is approached.

In this paper, a procedure for reducing the oscillations is proposed and investigated. Two case studies are examined; an axisymmetric model, previously investigated for one phase by Gonzalez Acosta et al. (2017), and a 2D plane strain consolidation problem.

PROPOSED METHOD FOR STRESS OSCILLATION REDUCTION

Two key causes of stress oscillations in MPM are cell crossing and the position of the material point for stress recovery. For both of these issues, the major problem arises from the use of the shape function (SF) gradients. If two-phase MPM is adopted, the rate of water pressure change is calculated as (Wang et al., 2018)

$$\dot{P}_w = \frac{K_w}{n}((1-n)\nabla v_s + n\nabla v_w) \tag{1}$$

where v_s is the velocity of the soil, v_w is the velocity of the water, n is the porosity of the soil, K_w is the water bulk modulus, and $\dot{P}_w$ is the incremental pore pressure. If the material point position and regular MPM (SF) gradients are used to compute nodal gradient velocities associated with the soil and water phases (∇v_s, ∇v_w), the results obtained are unrealistic, leading to an inaccurate estimation of the pore pressure. Moreover, considering the large bulk modulus of the water, the unrealistic pore pressure increases abruptly, causing element locking.

To reduce the recovery of unrealistic stresses in the two-phase approach, two features are included in the calculations. Initially, the GIMP method (Bardenhagen and Kober, 2004) was implemented and used to integrate the effective stresses and pore pressures using the material points, and also to recover effective stresses at the material points. By doing so, the water and soil velocities at the nodes improve considerably since the element crossing error is drastically reduced. Nevertheless, large pore pressure oscillations remain inside the elements. Hence, to avert such unrealistic pore pressures, a reduced integration has been adopted (GIMP-R) for pore pressure recovery, while the effective stresses are still calculated at material point locations using GIMP. With the reduced integration, the pore pressure increment is computed using a single Gauss point position at the centre of each element and then transferred to the material points inside the element.

BENCHMARK ANALYSES

To illustrate the unrealistic stresses that can be obtained in one- or two-phase problems, two examples are considered and analysed using regular MPM and GIMP-R. In both cases, an explicit version of MPM following Jassim et al. (2013) was used.

The first problem consists of an elastic axisymmetric benchmark problem. In this benchmark, an internal pressure is applied to the internal boundary of a hollow cylinder by means of prescribed loading. Figure 1 shows the geometry and boundary conditions. The distances between the inner and outer boundaries of the cylinder and the axisymmetric axis are $r_i = 0.20$ m and $r_e = 1.20$ m, respectively, giving a cylinder wall thickness of 1.0 m. The element size used to discretise the domain is $\Delta r = \Delta y = 0.20$ m. The internal prescribed loading is $F = 100.0$ kPa. The mechanical properties are an elastic modulus of $E = 1000.0$ kPa, and a bulk modulus of the water of $K_w = 2.2$ GPa. Two studies were performed, for Poisson's ratios of 0.2 and 0.49. Regarding the boundary conditions, the nodes at the top and bottom of the domain were allowed to move only in the radial direction, whereas the nodes at the outer boundary were fully fixed. The hydraulic conductivity was 1.0×10^{-4} m/s, and the domain did not allow the water to flow in or out, in order to simulate undrained conditions. The benchmark was solved by applying the internal pressure, and erasing the displacements, velocities and accelerations of the material points at the end of each step to avoid the interference of multiple elastic waves. A single phase solution was also calculated for comparison. The solution was obtained using a time step size of 1.0×10^{-6} s and a fully elastic analysis.
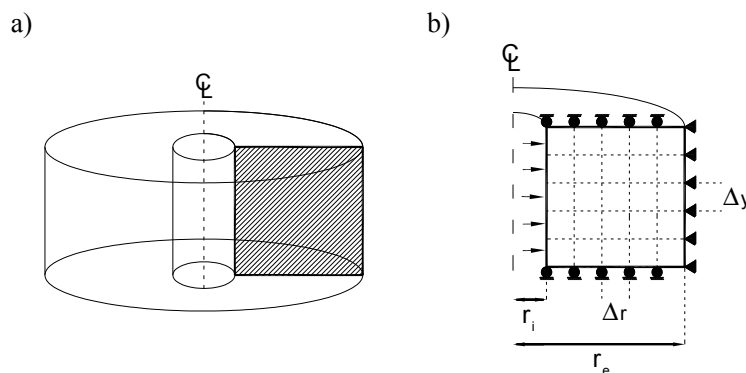

Figure 1 Benchmark axisymmetric problem.(a) General geometry, and (b) discretization of the cylinder wall

In Figure 2, the total radial stresses for each solution are shown. For single phase problems (as shown in Figure 2(a)), large stress oscillation using MPM are observed. For the soil with $v = 0.49$, i.e. a nearly incompressible material, the oscillations become even larger, and the radial total stresses for elements near to the external surface are smaller than the analytical solution. This is because the stress cannot propagate properly through the domain due to the locking of elements. When using GIMP-R to analyse this problem, it can be observed that the computed stresses at the element centres match quite well with the analytical solution. This further verifies the validity of the

GIMP-R procedure in mitigating the stress oscillations.

When considering two-phase problems (as shown in Fig. 2(b)), compared to the results for the one-phase cases (Figure 2(a)), larger oscillations are observed and they are almost the same for both Poisson's ratios considered. The reason is that drainage is not allowed and the stresses are ruled mainly by the water phase rather than the solid skeleton; since the water is almost incompressible, stress oscillations are larger. In addition, the results obtained using GIMP-R show almost constant values through the cylinder wall and these are identical to the external load, which is expected for incompressible materials. Using GIMP-R, the pore pressure is computed at the single Gauss point position and inaccurate pore pressures at the material point position are avoided.
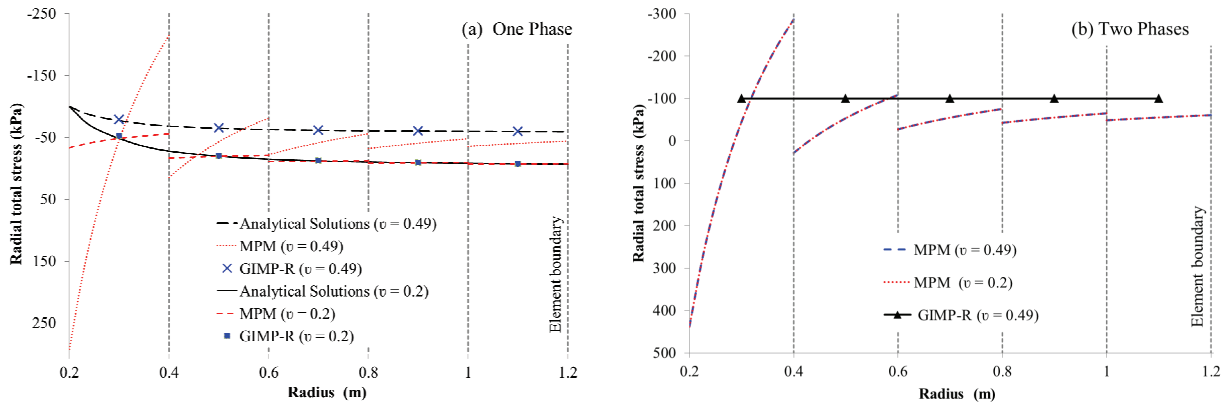

Figure 2 Radial total stress through the cylinder wall using (a) one- and (b) two-phase approaches with MPM and GIMP-R

The second problem consists of a two dimensional plane strain foundation soil subjected to an external surface load (F). In Figure 3a, the geometry of the problem and the initial boundary conditions are shown. In this case, the height of the domain is $H = 5$ m, and the width is $L = 5$ m. The left and right boundaries are allowed to move only in the vertical direction, and the base is totally fixed. The bottom boundary and two sides are assumed to be impermeable, and the pore water is only allowed to drain out from the top surface. The element size is $\Delta x = \Delta y = 0.50$ m. The external load is applied gradually on top of 3 surface elements until a maximum of $F = 1000$ kPa at time $t_p = 0.1$s with a time step size of 1.0×10^{-5}s (as shown in Figure 3b) and then kept constant. Again, the analysis is fully elastic with a Poisson's ratio of $v = 0.49$, an elastic modulus of $E = 10000$ kPa, a porosity of $n = 0.3$, a hydraulic conductivity of 1.0×10^{-4} m/s, and a bulk modulus of $K_w = 2.2$ GPa.
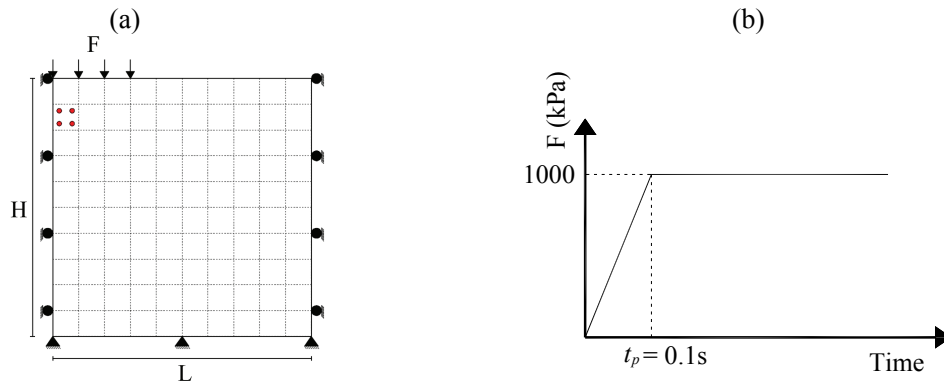

Figure 3 (a) Strip foundation on an elastic soil, and (b) external load applied

In Figure 4, the pore pressure distributions using both approaches are shown. In Figures 4a and 4d, the initial hydrostatic state is plotted, in which the pore pressure is due only to the gravitational force. In this case, the pore pressure distribution is the same for both cases. Then, in Figures 4b-c, the pore pressures computed by regular MPM at 0.1 and 1.0 seconds are plotted, revealing large stress oscillations and a typical checkerboard pattern due to locking. It is seen that both negative and positive pore pressures co-exist inside each background element. In Figure 4e-f, the pore pressures computed by GIMP-R are shown. In this case, the maximum pore pressure is drastically reduced (with respect to MPM), from -6800 kPa to -470 kPa, and the minimum is reduced from 5000 kPa to -15 kPa. In this case, there are no positive pore pressures, and the checkerboard pattern is not present.

Moreover, during the calculation, although material points cross element boundaries, large oscillations are not evident. On the other hand, using regular MPM the elements lock, and consequently there is no element boundary crossing.
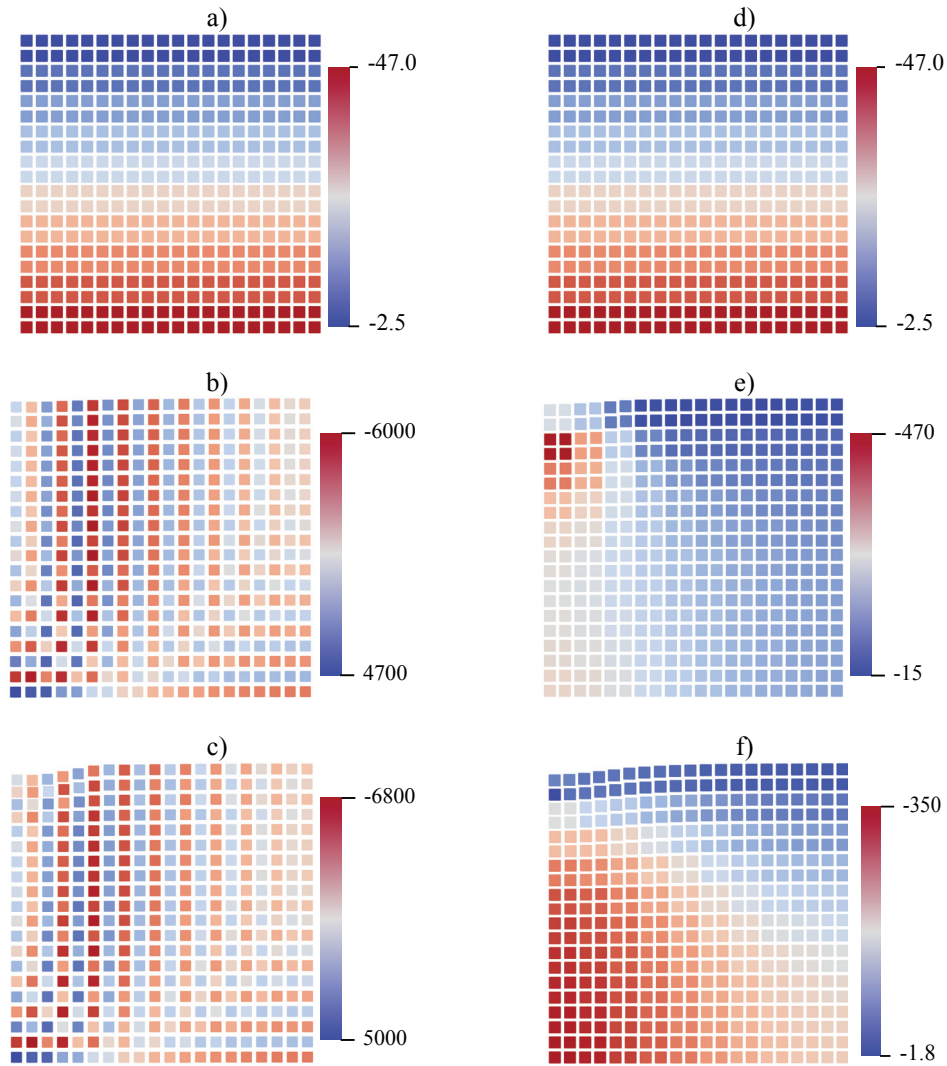
Figure 4 Pore pressures (in kPa) at time 0.0 s, 0.1 s and 1.0 s using regular MPM (a, b and c), and GIMP-R (d, e and f)
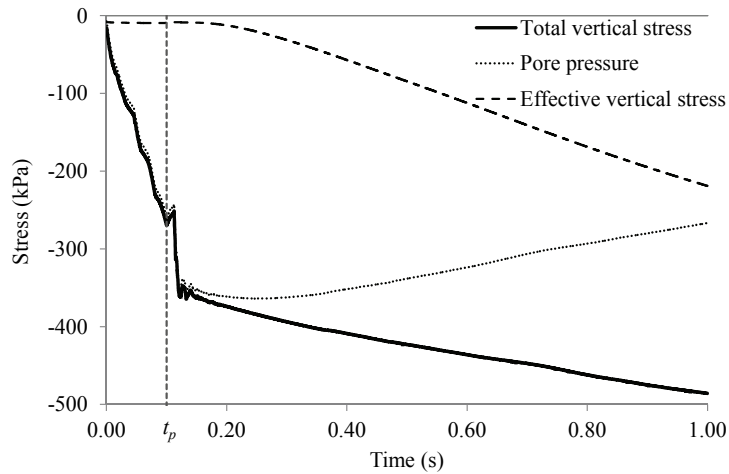
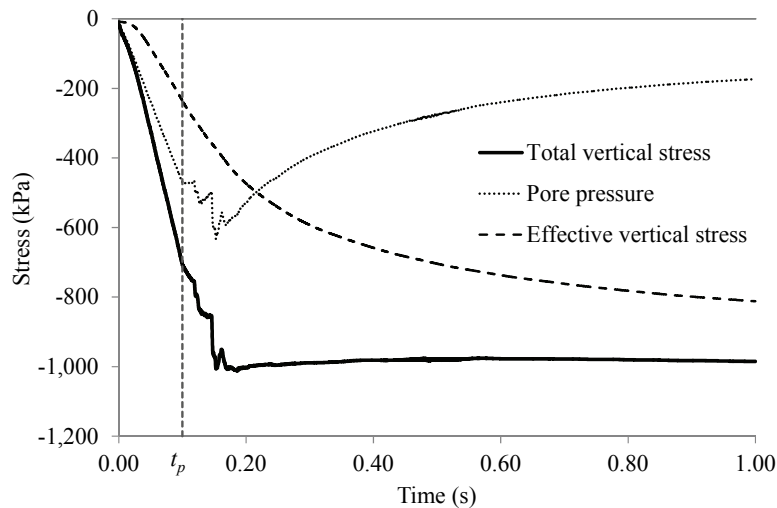Figure 5 Average stresses using regular MPM

Figure 6 Average stresses using GIMP-R

Finally, in Figures 5 and 6, the average stresses from the group of 4 material points shown in Figure 3a are plotted, for regular MPM and GIMP-R, respectively. If regular MPM is used (Figure 5), there is a slow increase of the effective stress and the total external load of 1000 kPa is not reached. However, if GIMP-R is used (Figure 6), the pore pressure oscillation is reduced and the total stress reaches the total external load.

CONCLUSIONS

This paper illustrates that the stress oscillation problem occurs even if material points do not cross element boundaries, and can become more severe if a hydro-mechanical (two-phase) approach is followed. The reason for such an increase in the stress oscillation without any material point crossing an element boundary, is that the stress distributions inside the elements are inaccurate and not constant, and this problem is magnified because of the incompressibility of the water, leading to element locking. If cell crossing occurs, the inaccuracies are more severe, especially when regular MPM is used. If the GIMP-R procedure is adopted, the pore pressure is computed at the single Gauss point position, for which the computed incremental pore pressure remains accurate. Then, the integration of stresses from material points to nodes is improved by using the GIMP shape function. The locking of elements is no longer observed and the typical checkerboard pattern disappears.

REFERENCES

Bardenhagen SG. (2002). Energy conservation error in the material point method for solid mechanics. *Journal of Computational Physics*, 180(1): 383–403.
Bardenhagen SG & Kober EM. (2004). The generalized interpolation material point method. *Computer Modeling in Engineering and Sciences*, 5(6): 477–495.
González Acosta JL, Vardon PJ & Hicks MA. (2017). An evaluation of MPM, GIMP and CMPM in geotechnical problems considering large deformations. *Proceedings of the 15th International Conference of the International Association for Computer Methods and Advances in Geomechanics*, Wuhan, China.
Jassim I, Stolle D & Vermeer, PA. (2013). Two-phase dynamic analysis by material point method. *International Journal for Numerical and Analytical Methods in Geomechanics*, 37(15): 2502–2522.
Steffen M, Kirby RM & Berzins M. (2008a). Analysis and reduction of quadrature errors in the material point method (MPM). *International Journal for Numerical Methods in Engineering,* 76(6): 922–948.
Steffen M, Wallstedt PC, Guilkey JE, Kirby RM & Berzins M. (2008b). Examination and analysis of implementation choices within the material point method (MPM). *Computer Modeling in Engineering and Sciences*, 31(8): 107–127.
Wang B, Vardon PJ & Hicks MA. (2018). Rainfall-induced slope collapse with coupled material point method. *Engineering Geology*, 239: 1–12.